Clinical Validation of a Machine-learning–derived Signature Predictive of Outcomes from First-line Oxaliplatin-based Chemotherapy in Advanced Colorectal Cancer

Jim P. Abraham[1], Daniel Magee[1], Chiara Cremolini[2], Carlotta Antoniotti[2], David D. Halbert[1], Joanne Xiu[1], Phillip Stafford[1], Donald A. Berry[3], Matthew J. Oberley[1], Anthony F. Shields[4], John L. Marshall[5], Mohamed E. Salem[6], Alfredo Falcone[2], Axel Grothey[7], Michael J. Hall[8], Alan P. Venook[9], Heinz-Josef Lenz[10], Anthony Helmstetter[1], W. Michael Korn[1], and David B. Spetzler[1]

ABSTRACT

Purpose: FOLFOX, FOLFIRI, or FOLFOXIRI chemotherapy with bevacizumab is considered standard first-line treatment option for patients with metastatic colorectal cancer (mCRC). We developed and validated a molecular signature predictive of efficacy of oxaliplatin-based chemotherapy combined with bevacizumab in patients with mCRC.

Experimental Design: A machine-learning approach was applied and tested on clinical and next-generation sequencing data from a real-world evidence (RWE) dataset and samples from the prospective TRIBE2 study resulting in identification of a molecular signature, FOLFOX*ai*. Algorithm training considered time-to-next treatment (TTNT). Validation studies used TTNT, progression-free survival, and overall survival (OS) as the primary endpoints.

Results: A 67-gene signature was cross-validated in a training cohort ($N = 105$) which demonstrated the ability of FOLFOX*ai* to distinguish FOLFOX-treated patients with mCRC with increased benefit from those with decreased benefit. The signature was predictive of TTNT and OS in an independent RWE dataset of 412 patients who had received FOLFOX/bevacizumab in first line and inversely predictive of survival in RWE data from 55 patients who had received first-line FOLFIRI. Blinded analysis of TRIBE2 samples confirmed that FOLFOX*ai* was predictive of OS in both oxaliplatin-containing arms (FOLFOX HR, 0.629; $P = 0.04$ and FOLFOXIRI HR, 0.483; $P = 0.02$). FOLFOX*ai* was also predictive of treatment benefit from oxaliplatin-containing regimens in advanced esophageal/gastro-esophageal junction cancers, as well as pancreatic ductal adenocarcinoma.

Conclusions: Application of FOLFOX*ai* could lead to improvements of treatment outcomes for patients with mCRC and other cancers because patients predicted to have less benefit from oxaliplatin-containing regimens might benefit from alternative regimens.

Introduction

The promise of precision cancer therapy has not yet been fully realized for patients with metastatic colorectal cancer (mCRC). Over the last 2 decades, conventional chemotherapies (e.g., oxaliplatin and irinotecan) and biologics (including bevacizumab, which targets VEGF, and cetuximab and panitumumab, which target EGFR) have shown activity in first-line treatment of mCRC. In combination with a fluoropyrimidine, the resulting chemotherapy doublets (FOLFOX and FOLFIRI) have each been found superior to the components (1) and have become standard of care, typically in combination with biologics. However, numerous studies have failed to clearly establish that any of these combination regimens would be superior for any individual patient based on clinical factors. Recently, results of the TRIBE2 phase III study (2) demonstrated that the upfront triple combination of 5-fluorouracil (5-FU), oxaliplatin, and irinotecan (FOLFOXIRI) with bevacizumab followed by the reintroduction of the same regimen after disease progression resulted in improved overall survival (OS) compared with the sequential administration of chemotherapy doublets (FOLFOX followed by FOLFIRI), in combination with bevacizumab (2). However, these improved outcomes were achieved at the cost of increased, clinically relevant toxicity, thus limiting broad applicability of this approach.

Since 2008, when the presence of *KRAS* mutations in a tumor was found to preclude benefit from antibodies targeting EGFR (3), it has been anticipated that multi-gene molecular profiling would further refine the ability to personalize treatment of mCRC. However, biomarkers relevant for first-line treatment decisions are limited to KRAS, NRAS, and *BRAF*, as well as microsatellite instability status (4–6). Efforts to identify biomarkers for chemotherapy in

[1]Caris Life Sciences, Phoenix, Arizona. [2]Departments of Oncology and Translational Research and New Technologies in Medicine, University Hospital Pisa, Pisa, Tuscany, Italy. [3]Department of Biostatistics, The University of Texas MD Anderson Cancer Center, Houston, Texas. [4]Department of Oncology, Karmanos Cancer Institute, Wayne State University, Detroit, Michigan. [5]Ruesch Center for The Cure of Gastrointestinal Cancers, Lombardi Comprehensive Cancer Center, Georgetown University Medical Center, Washington, D.C. [6]Levine Cancer Institute, Carolinas HealthCare System, Charlotte, North Carolina. [7]Medical Oncology, West Cancer Center, Germantown, Tennessee. [8]Department of Clinical Genetics, Fox Chase Cancer Center, Philadelphia, Pennsylvania. [9]Division of Hematology/Oncology, Department of Medicine, University of California San Francisco, San Francisco, California. [10]University of Southern California, Keck School of Medicine, Norris Comprehensive Cancer Center, Los Angeles, California.

Note: Supplementary data for this article are available at Clinical Cancer Research Online (http://clincancerres.aacrjournals.org/).

Corresponding Authors: David B. Spetzler, Caris Life Sciences (United States), 4610 South 44th Place, Phoenix, AZ 85040. Phone: 602-464-7601; Fax: 602-464-7661; E-mail: dspetzler@carisls.com; and W. Michael Korn, E-mail: wmkorn@carisls.com

Clin Cancer Res 2021;27:1174–83

doi: 10.1158/1078-0432.CCR-20-3286

Translational Relevance

FOLFOX, FOLFIRI, or FOLFOXIRI chemotherapy in combination with bevacizumab is considered standard first-line treatment option for patients with metastatic colorectal cancer. To determine whether benefit from first-line chemotherapy in colorectal cancer is predictable, we leveraged artificial intelligence algorithms and comprehensive molecular profiling data to identify and validate a predictor of benefit from FOLFOX chemotherapy. A 67-gene signature was predictive of survival in an independent real-world evidence (RWE) dataset of 412 patients who had received FOLFOX/bevacizumab in first line and inversely predictive of outcomes in RWE data from 55 patients who had received first-line FOLFIRI chemotherapy. Blinded analysis of TRIBE2 samples confirmed that FOLFOX*ai* was predictive of overall survival in both oxaliplatin-containing arms (FOLFOX HR, 0.629; $P = 0.04$ and FOLFOXIRI HR, 0.483; $P = 0.02$). FOLFOX*ai* was also predictive of benefit from oxaliplatin-containing regimens in advanced esophageal/gastro-esophageal junction cancers, as well as pancreatic ductal adenocarcinoma.

mCRC have been even less fruitful than for the biologics. Genetic polymorphisms in metabolizing enzymes may explain toxicities of fluoropyrimidines and irinotecan, but are of limited clinical value. Topoisomerase levels have been shown to be unhelpful when considering irinotecan activity, as have VEGF-A serum levels for bevacizumab (7).

The vast majority of patients with mCRC receive FOLFOX-based first-line treatment, even though neuropathy almost always limits its use beyond 4 months. Oxaliplatin has also become a first-line option as part of FOLFOXIRI in mCRC (2) and for other cancers, including FOLFOX in first-line esophageal and gastric cancer (8), and as part of FOLFIRINOX in advanced pancreatic cancer (9). Given other choices in these diseases, a biomarker predicting the relative efficacy of these regimens would be very helpful. Because oxaliplatin has little activity as monotherapy (1), it is used exclusively in combination with fluoropyrimidines, so a biomarker for FOLFOX (as opposed to oxaliplatin alone) would be of pertinent clinical value. The urgent need for predictive biomarkers is highlighted by the fact that a randomized study conducted in 376 patients demonstrated that tumor expression of the excision repair cross-complementing-1 gene (*ERCC-1*) is not a valid predictor of oxaliplatin efficacy in mCRC (7).

Business as usual has not worked in the pursuit of these biomarkers. The routine application of comprehensive molecular profiling, in particular involving next-generation DNA sequencing, has allowed for the creation of increasingly refined molecular portraits of large numbers of tumors from a diverse and representative patient pool (10). Systematic molecular analyses of colorectal cancers have demonstrated extensive inter- and intratumoral heterogeneity and, at the same time, have led to the identification of subclasses of the disease with different prognostic and therapeutic characteristics (11). Although most of the currently available studies have utilized conventional statistics for disease subclassification, recent advances in machine learning enable identification of nonintuitive and nonlinear patterns and hold the promise of supporting diagnostic and therapeutic decision-making with high accuracy.

The availability of large, combined clinical and molecular datasets enables development of novel molecular predictors of efficacy of standard treatments. Here, we report the results of a machine-learning approach in an attempt to identify a molecular signature predictive of clinical benefit from FOLFOX chemotherapy in previously untreated patients with mCRC. We then sought validation of the putative molecular signature from a large real-world evidence (RWE) database, a subset of cases from the randomized controlled phase III TRIBE2 study, as well as RWE data from patients with advanced esophageal/gastro-esophageal junction cancers (EC/GEJC) or pancreatic ductal adenocarcinoma (PDAC) who received first-line treatments with oxaliplatin-containing regimens.

Materials and Methods

RWE and TRIBE2 clinical trial cohorts

We utilized an extensive deidentified RWE outcomes dataset collected from the Caris Life Sciences Precision Oncology Alliance registry, and insurance claims data from more than 10,000 physicians. The following inclusion criteria were applied for selecting the training cohort: (i) diagnosis of mCRC, (ii) treatment with FOLFOX-based combination therapy, (iii) completion of at least one full cycle of therapy, and (iv) completed next-generation DNA analysis of at least one colorectal cancer sample using a 592-gene panel. Patients were excluded if they had prior chemotherapy, including adjuvant therapy. Two separate RWE validation cohorts were generated using the following inclusion criteria: (i) diagnosis of mCRC, (ii) first-line FOLFOX/bevacizumab treatment (FOLFOX/bevacizumab cohort) or first-line FOLFIRI-based treatment (FOLFIRI cohort), (iii) completion of at least one full cycle of therapy, (iv) completed next-generation DNA analysis of at least one colorectal cancer sample using a 592-gene panel, and (v) switch to an irinotecan-containing regimen (FOLFOX/bevacizumab cohort) or to FOLFOX (FOLFIRI cohort). Inclusion criteria for the FOLFOX/bevacizumab cohort were modeled after the TRIBE2 study protocol.

A blinded retrospective-prospective analysis of samples from patients enrolled in the phase III TRIBE2 study, with completed next-generation sequencing (NGS) analysis, was performed for further clinical validation. The trial, conducted by the Italian Gruppo Oncologico del Nord-Ovest (GONO), compared the upfront exposure with FOLFOXIRI/bevacizumab followed (after maintenance therapy of 5-FU/bevacizumab) by the reintroduction of the same regimen to a preplanned sequential strategy of FOLFOX/bevacizumab followed by FOLFIRI/bevacizumab after disease progression in the treatment of patients with mCRC. Detailed eligibility criteria and results have been reported previously (2). All personnel at Caris Life Sciences were blinded to any clinical data associated with these samples. The samples in this trial were subjected to the same quality controls and genomic testing protocols as cases from the RWE training and testing cohorts and outcome predictions for these cases were returned to GONO for unblinding and assessment of the model's performance. In addition, exploratory analyses were performed in RWE cohorts for patients with metastatic PDAC who had received either nab-paclitaxel/gemcitabine or FOLFIRINOX as first-line treatment regimen and patients with metastatic or unresectable esophageal or gastroesophageal adenocarcinoma who had been treated with FOLFOX as first-line treatment regimen. Therapy records for all patients included in the RWE dataset were curated by a board-certified medical oncologist prior to inclusion in the study.

Time-to-next treatment

Time-to-next treatment (TTNT) was defined as the time from first administration of oxaliplatin or 5-FU following the biopsy or surgical specimen collection to the first administration of irinotecan

(indicating a switch to FOLFIRI) or last contact. Patients were algorithmically identified using this method, followed by manual curation by a board-certified medical oncologist to ensure that a FOLFOX regimen had been used appropriately and that the TTNT value was accurate. For algorithm training, a TTNT of 270 days was chosen to define whether a patient benefitted from receiving first-line FOLFOX based on the progression-free survival (PFS) noted by Tournigard and colleagues of approximately 8.5 months (12) and approximately 30 days less than the PFS in the MAVERICC study (7). Training cases were required to have at least 270 days of follow-up after beginning the FOLFOX regimen, if there was no observable switch to FOLFIRI (i.e., short-censored cases). We referred to patients with TTNT < 270 days as having decreased benefit (DB) to FOLFOX and others as having increased benefit (IB).

Overall survival

Overall survival (OS) was calculated for all eligible cases, which was defined as the time from treatment initiation date to either death for the RWE dataset [from the National Death Index (NDI), National Center for Health Statistics, Centers for Disease Control and Prevention] or last contact in the insurance claims repository. We assumed that any patient without a claim for more than 100 days had died, which holds true for more than 95% of patients with a recorded death in the NDI. Conversely, patients with a last contact date within 100 days of the most recent refresh of the RWE repository were censored. With regard to the TRIBE2 analysis, OS was defined as time from randomization to death.

Kaplan–Meier metrics

All listed HRs use the Cox proportional hazards model and the *P* values were calculated using the log-rank statistic. To test whether the signature predicts the same survival benefit for different first-line therapies, we generated a Cox proportional hazards model on the combined RWE cohorts for either mCRC, PDAC, or EC/GEJC using the model prediction, first-line treatment, and an interaction term between first-line treatment and predicted benefit as covariates. To visualize the effect of the interaction between DB probability and first-line treatment, we used the fitted Cox model to predict relative risk on simulated data using first-line treatment information.

Tumor samples and NGS

Tumor containing formalin-fixed, paraffin-embedded blocks from surgery or biopsy prior to administration of any chemotherapy were used to generate all genomic data used in all analyses as described previously (13). The genomic data have been deposited in an open-access GitHub repository and are available at https://github.com/carisls/Abraham_2020.

Algorithm ensemble and model selection

Genomic features obtained via the Caris Life Sciences 592-gene NGS panel were used as feature inputs into an ensemble of more than 300 published machine-learning algorithms, including random forest, support vector machine, logistic regression, K-nearest neighbor, artificial neural network, naïve Bayes, quadratic discriminant analysis, and Gaussian processes models. Multiple feature selection methods, including principal component analysis, mutual information, and variable importance, were employed to build models that predict IB or DB to first-line FOLFOX chemotherapy. The final algorithm returned an IB probability obtained from a consensus of model predictions, which decreases the dependence on individual fixed decision trees.

Performance of all machine-learning models was implemented by using the Python package, scikit-learn v0.22.1. Biomarker data obtained via NGS for the 105 patients in the training cohort were used as features to classify each patient based on their binary IB or DB status, defined by TTNT ≥ 270 days, as described previously. We analyzed the performance of models on the training data via 5-fold cross-validation, selected because of the relatively small sample size, on metrics including HR, sensitivity, specificity, positive and negative predictive values, and overall accuracy. Emphasis was placed on correctly identifying the patients with the longest and shortest TTNT due to the obvious clinical implications of misclassifying them. With respect to HR and the log-rank *P* value, predictions on the five hold-out folds were combined and this metric was measured once per iteration to avoid possibly misleading values due to low *N* (21/fold). Models were trained on both the full biomarker set, as well as smaller feature sets after applying various feature selection methods. For example, we used variable importances across folds in tree-based methods, like random forests, to establish the biomarkers that are most essential to correct classification. The feature set was then trimmed to only include the most important biomarkers, and the same model was retrained and cross-validation metrics were evaluated. The performance improvement, or lack thereof, using the smaller dataset helped reveal whether the culled features were introducing noise that negated our ability to successfully classify the IB and DB cohorts. An exhaustive search using this method, where each individual machine-learning algorithm was allowed to independently select features and tune hyperparameters, yielded five random forest configurations that were able to effectively and consistently separate the IB and DB cohorts without demonstrating statistical differences in mutation frequencies of prognostic variables, such as BRAF or the sidedness of the tumor. The algorithms were also evaluated for their ability to predict response in patients that received first-line FOLFIRI in addition to the primary FOLFOX training cohort. Models that exhibited similar HRs in the FOLFOX and FOLFIRI cohorts were discarded as they were likely driven by prognostic factors, and features that enabled such performance were penalized or removed during additional model training. These findings in the training data suggested that our algorithms may be predictive of FOLFOX response and would extrapolate well onto the testing dataset without demonstrating potentially confounding biases. We then focused on establishing a single, aggregated prediction for each patient using the five individual classifiers.

To address ambiguity or disagreement among models for any given patient, we employed a voting scheme. Without being bound by theory, each model may perform optimally on cases having different characteristics, and in combination the voting scheme accounts for suboptimal or supraoptimal performance of any given model on a subset(s) of cases. To achieve a consensus and reduce subtle noise implemented by any individual random forest model, we trained 1,000 instances of each of the five model configurations for a total of 5,000 models. Each of these models were used to vote on the consensus prediction for all patients in the validation cohorts and return a probability of IB using our deliberative analytics (DEAN) framework. The DEAN framework evaluates multiple approaches for reaching a consensus, ranging from simple aggregations to sophisticated machine-learning models. For FOLFOX, the median of the model probabilities provides the optimal result. To further account for model noise, we introduced a buffer surrounding the 50% IB probability threshold in which cases were considered a "no call." We chose this threshold by observing the IB probability range for each patient in this study. A 3% buffer was selected as it is one SD larger than the mean range, so the model will not return a prediction if the IB probability

falls within 47%–53%. At this time, the locked ensemble predictor was graduated to the testing phase and was applied to the additional RWE and TRIBE2 data. We referred to our patent for full details of the machine-learning configurations and inputs (14).

Assessment of predictive versus prognostic nature of the model

To test whether the signature was merely prognostic, we generated a Cox proportional hazards model on the combined set of RWE patients that received either first-line FOLFOX or first-line FOLFIRI for mCRC and FOLFIRINOX or nab-paclitaxel/gemcitabine for PDAC. The EC/GEJC cohort was excluded from this analysis as only one first-line therapy was included in this work. Three terms were included in the Cox model: first-line treatment, predicted benefit (IB or DB), and an interaction term between first-line treatment and predicted benefit. An additional three-term Cox proportional hazards model was fit on the same cohort, with the binary IB/DB prediction replaced with the continuous valued probability of DB from the model. To visualize the effect of the interaction between DB probability and first-line treatment, we used the fitted Cox model to predict RR on simulated data, where DB probability ranged from 0.01 to 0.99, once with FOLFOX as the first-line treatment and again with FOLFIRI as the first-line treatment for mCRC and similarly FOLFIRINOX or nab-paclitaxel with gemcitabine for PDAC.

Consensus molecular subtype classification

A consensus molecular subtype (CMS) classifier was developed using expression values obtained from deidentified RNA sequencing (RNA-seq) data from routine testing at the Caris Life Sciences Laboratory allowing for classifying colorectal cancers into four subtypes analogous to Guinney and colleagues (10). A full 22,948-gene dataset of expression data was produced by the Salmon RNA-seq pipeline (15), which provides fast and bias-aware quantification of transcript expression. This pipeline yields discrete transcripts per million molecules values for each gene transcript. A classifier was trained against the original CMS datasets, as published by Guinney and colleagues (11), using a classic SVM model as implemented in R. The Cancer Genome Atlas (TCGA) dataset of 512 cases was excluded from training. Six-hundred genes were subsequently selected for each of the four CMS classifiers using one versus all *t* test to identify genes uniquely expressed in each of the four classes. Cross-validation was performed to optimize the model and finalize SVM parameters. Possible overtraining was evaluated by predicting CMSs from an independent blinded TCGA dataset (512 samples; ref. 11), with an accuracy of 88.3%.

Compliance statement

The study was conducted in accordance with the Declaration of Helsinki and adhered to Good Clinical Practice guidelines. Molecular analyses were performed in a Clinical Laboratory Improvements Amendments–approved laboratory. Approval was obtained from the local ethics committees of participating sites, and all TRIBE2 patients provided written informed consent to participate in the study, while the RWE analysis was performed on deidentified data. This part of the

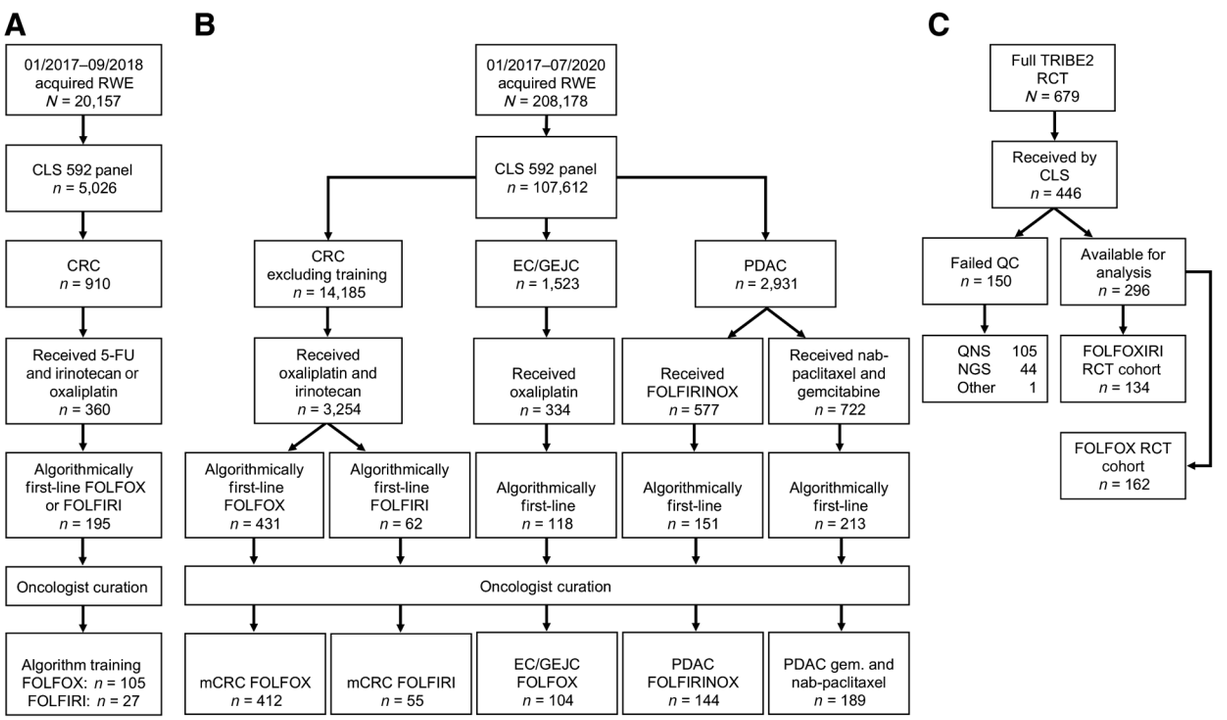

Figure 1.

Consort diagram of selection of patients on which to train and cross-validate the FOLFOX*ai* model (**A**), RWE testing data (**B**), TRIBE2 randomized phase III cases (**C**). Outcomes in **A** were last refreshed in September 2018 and outcomes in **B** were last refreshed in July 2020. The FOLFOX*ai* algorithm was locked in December 2018, more than 9 months before receiving the outcomes associated with **B**. CRC, colorectal cancer; CLS, Caris Life Sciences; QC, quality control; QNS, quantity not sufficient; RCT, randomized controlled trial.

Table 1. Demographics of the cases used in the mCRC RWE testing set.

	First-line FOLFOX							First-line FOLFIRI						
	Actual			Model prediction				Actual			Model prediction			
Characteristic	DB	IB	*P*[a]	DB	No call	IB	*P*[a]	DB	IB	*P*[a]	DB	No call	IB	*P*[a]
Number of patients	179	233		120	50	242		26	29		20	6	29	
Mean age (range)	58.0 (31–85)	57.9 (22–86)	0.93	57.5 (33–78)	56.6 (31–80)	58.5 (22–86)	0.44	60.9 (26–85)	55.3 (32–77)	0.09	56.0 (32–77)	62.8 (53–79)	58.4 (26–85)	0.47
Gender (F/M, %)	45/55	42/58	0.73	43/57	48/52	43/57	0.78	27/73	48/52	0.18	35/65	33/67	41/59	0.87
Primary tumor site, %[b]	44/38/18	53/29/18	0.13	52/36/12	52/36/12	48/31/21	0.21	35/54/12	62/21/17	0.04	65/30/5	83/17/0	31/45/24	0.04
BRAF, %[c]	91/1/9	97/0/3	0.02	92/0/8	98/2/0	94/0/6	0.03	100/0/0	90/3/7	0.24	90/5/5	83/0/17	100/0/0	0.20
KRAS, %[c]	45/1/54	41/0/59	0.36	42/0/58	36/2/62	45/0/55	0.07	42/0/58	28/0/72	0.39	25/0/75	50/0/50	38/0/62	0.45
MSI, %[d]	92/7/2	91/9/0	0.35	84/13/2	92/6/2	95/5/0	<0.01	96/4/0	97/3/0	1.00	95/5/0	100/0/0	97/3/0	0.85
Second-line EGFRi, %[e]	74/26	71/29	0.59	76/24	74/26	70/30	0.46	88/12	72/28	0.25	75/25	83/17	83/17	0.78

Abbreviation: EGFRi, EGFR inhibitor.
[a]χ^2 tests were used for categorical variables and Mann–Whitney U for nonnormally distributed age data.
[b]Left/right/unknown or mix.
[c]No pathogenic variant detected/indeterminate/pathogenic variant detected.
[d]Stable/indeterminate/high.
[e]No/yes.

study was exempt from consent requirement as per review by the Western Institutional Review Board.

Results

Patients

The training cohort consisted of 105 patients with mCRC from the RWE dataset who had received first-line FOLFOX-based treatment and who had been profiled by Caris Life Sciences (**Fig. 1**). IB and DB cohorts were well balanced in terms of age, gender, tumor location (left and right), mutation status, and biologic agent administered in combination with chemotherapy (Supplementary Table S1). The first independent validation cohort included 412 patients (with RWE data on treatments and death dates) treated with FOLFOX/bevacizumab and 55 patients who had received FOLFIRI as first-line treatments (**Fig. 1**). Of the FOLFIRI patients, 82% received bevacizumab, 9% panitumumab, and 5% cetuximab, respectively, while 4% (two patients) did not receive a combination with a biologic. In all RWE cohorts, IB, no call, and DB groups were well balanced in terms of key prognostic features, including age, gender, tumor location (left and right), *KRAS/NRAS/BRAF* mutation status, and microsatellite status (**Table 1**). Additional RWE datasets included 333 patients with advanced PDAC and EC/GEJC treated in first line with oxaliplatin-containing regimens (**Fig. 1B**; Supplementary Tables S2 and S3). Patients with PDAC in the nab-paclitaxel/gemcitabine group were significantly older than patients in the FOLFIRINOX group (68.4 vs. 59 years; $P < 0.0001$), in agreement with current prescribing practices. Comparison of the characteristics of the 296-patient subset from the TRIBE2 trial, for whom complete NGS tumor analyses were available (**Fig. 1**), demonstrated that the subset was representative of the entire study population (**Fig. 1C**; Supplementary Table S4). Samples from 25 patients in this set of samples did not meet the minimum quality metric (sequencing depth requirement of 300×).

Model training and validation in RWE cohorts

The RWE cohort did not include PFS, therefore, we used TTNT instead. We compared TTNT and PFS within the TRIBE2 samples in both the FOLFOX (Pearson $r = 0.98$) and FOLFOXIRI ($r = 0.99$) arms of the trial (Supplementary Fig. S1A) and found them to be highly correlated. Model training was done using TTNT on a patient cohort that included 63 patients with IB and 42 with DB, based on our benefit definition (Materials and Methods). Results of 5-fold cross-validation demonstrated that the model consistently separated IB from DB cohorts [median HR, 0.398 for 100 model cross-validations; 95% confidence interval (CI), 0.244–0.649; log-rank $P < 0.001$; Supplementary Fig. S2]. The final model took 67 genes into account (**Table 2**). Among the most relevant features included in the signature were genes involved in mediating WNT signaling (*BCL9* and *CDX2*), epithelial-to-mesenchymal transition (EMT; *INHBA, PRRX1, PBX1*, and *YWHAE*), chromatin remodeling (*EP300, ARID1A, SMARC4*, and *NSD3*), DNA repair (*WRN* and *BRIP1*), NOTCH signaling (*MAML2*), and cell-cycle regulation (*CNTRL* and *CCNE1*). After locking the algorithm, further validation of the predictive signature (named FOLFOX*ai*) was performed in the FOLFOX/bevacizumab cohort (**Fig. 1**).

No call was made if the model output, interpretable as DB probability, was between 0.47 and 0.53 (Materials and Methods), which was the case in 50 patients (12.1%; **Fig. 3**). There were 242 patients in the IB cohort and 120 in the DB cohort who are well balanced in terms of known prognostic features, with the exception

Table 2. List of genomic features used in the algorithm.

ACKR3	BRIP1	EWSR1	IL2	MSI2	PRRX1	TOP1
AKT2	CASP8	EZR	INHBA	MYC	RUNX1T1	TRRAP
AKT3	CCNE1	FAS	KEAP1	NFIB	SBDS	U2AF1
ARFRP1	CDX2	FCRL4	LHFPL6	NFKBIA	SDC4	WRN
ARID1A	CNTRL	FH	LMO1	NSD3	SEPT5	WWTR1
ASXL1	COX6C	FLT1	MAML2	PAX7	SMARCA4	YWHAE
AURKA	CREB1	FLT3	MAP2K4	PBX1	SOX10	ZNF217
BCL9	CRKL	GAS7	MLF1	PCM1	TCL1A	
BIRC3	EP300	GNAS	MN1	PDGFB	TERT	
BRD3	ETV6	HOXA11	MNX1	PER1	TLX3	

of a higher representation of tumors with indeterminate/high microsatellite instability (MSI) status in patients with predicted DB (**Table 1**). Kaplan–Meier analysis demonstrated a significant difference in TTNT and OS on the basis of the predicted IB or DB, respectively (median TTNT of 11.5 months for IB and 8.2 months for DB; HR, 0.537; 95% CI, 0.428–0.674; log-rank $P < 0.0001$; **Fig. 2A** and median OS of 42 months for IB and 24.5 months for DB; HR, 0.466; 95% CI, 0.325–0.670; log-rank $P < 0.0001$; **Fig. 2B**). To analyze specificity of FOLFOX*ai*, we applied the predictor to the FOLFIRI cohort. In contrast to the FOLFOX/bevacizumab cohort, the signature prediction resulted in inverted survival curves in the FOLFIRI cohort: patients predicted to have DB from FOLFOX had significantly better outcomes than those with predicted IB and vice versa. The median OS was 18.7 months for IB and 34.4 months for DB (HR, 2.631; 95% CI, 1.041–6.649; log-rank $P = 0.034$; **Fig. 2C** and **D**). A multivariate Cox proportional hazards model was performed using all FOLFOX and FOLFIRI patients (Materials and Methods). A third-line therapy was present in 25% of FOLFOX and 22% of FOLFIRI patients, primarily in the form of trifluridine and tipiracil (Lonsurf) or regorafenib. With respect to time to third treatment, the FOLFOX cohort predicted as IB showed improvement over the predicted DB cohort (HR, 0.429; $P < 0.0001$), while the FOLFIRI cohort did not show statistical significance (HR, 1.680; $P = 0.20$). The interaction between the treatment and prediction covariates showed statistical significance so we rejected the null hypothesis that FOLFOX*ai* predicts the same OS benefit for both the FOLFOX and FOLFIRI cohorts (**Fig. 2I** and **J**; Supplementary Table S5).

We next asked whether FOLFOX*ai* was predictive of treatment efficacy of oxaliplatin-containing regimens in other disease. To address this possibility, similar analyses were conducted in the PDAC and EC/GEJC cohorts. These analyses demonstrate that the signature was indeed predictive of OS in the FOLFIRINOX, with a median OS improvement of 10.1 months in the IB cohort (21.4 months for IB and 11.3 months for DB; HR, 0.478; CI, 0.289–0.792; log-rank $P = 0.003$), but not the nab-paclitaxel/gemcitabine cohort (median OS, 10.8 months for IB and 9.8 months for DB; HR, 0.958; CI, 0.658–1.395; log-rank $P = 0.823$; Supplementary Fig. S3A and S3B). Like FOLFOX and FOLFIRI for mCRC, the Cox proportional hazards covariate for the interaction between first-line PDAC therapy and FOLFOX*ai* prediction yielded $P = 0.03$, so we again rejected the null hypothesis that the FOLFOX*ai* prediction provides the same OS benefit for both the FOLFIRINOX and nab-paclitaxel/gemcitabine cohorts (Supplementary Table S5). Similarly, data from 104 patients with advanced EC/GEJC demonstrated that FOLFOX*ai* was predictive of efficacy of oxaliplatin-containing regimens also in this clinical setting (median OS for IB, 14 months and DB, 8.9 months; HR, 0.437; CI, 0.250–0.763; log-rank $P = 0.003$; Supplementary Fig. S3C). These results demonstrate specificity and potential of FOLFOX*ai* for broad clinical applicability.

Blinded retrospective-prospective analysis of the TRIBE2 study

Data and samples from 271 patients were available for analysis from the TRIBE2 study. IB versus DB was predicted for 97 versus 36 patients on the FOLFOX/bevacizumab arm and 83 versus 20 patients on the FOLFOXIRI arm, respectively. No call was made by the predictive algorithm in 35 (12.9%) patients (Materials and Methods). Median PFS1 for patients with IB was 0.9 months longer than for patients with DB (9.6 vs. 8.7 months; HR, 0.757; 95% CI, 0.505–1.135; log-rank $P = 0.18$; **Fig. 2E**) and the median OS difference was 6 months (24.8 vs. 18.7 months; HR, 0.629; 95% CI, 0.404–0.981; log-rank $P = 0.04$; **Fig. 2F**) in the FOLFOX/bevacizumab arm. The differences were also significant in the FOLFOXIRI/bevacizumab arm for OS (PFS1, 13.8 vs. 7.6 months; HR, 0.683; CI, 0.396–1.181; log-rank $P = 0.17$; **Fig. 2G** and OS, 30 vs. 15.9 months; HR, 0.483; CI, 0.270–0.864; log-rank $P = 0.02$; **Fig. 2H**). Thus, this blinded retrospective-prospective analysis of the samples from the TRIBE2 trial confirms the signature differentiates IB versus DB in terms of PFS and OS in patients receiving FOLFOX or FOLFOXIRI in combination with bevacizumab.

Overlap with colorectal cancer CMSs

Investigations into differences in RNA expression profiles in colorectal cancer have revealed four distinct colorectal molecular subtypes (CMS1–4) that are associated with different prognoses and possibly response to chemotherapies and biologic therapies (11, 16, 17). To assess whether FOLFOX*ai* merely reproduced this classification, we first validated the Caris whole transcriptome sequencing–based CMS classifier using 2,224 whole transcriptome sequencing profiles available in the Caris database. The classifier assigned a CMS class to the samples analyzed with similar frequency distribution and molecular characteristics as the published, expression array–based classifier (11). Next, we calculated both CMS classification, as well as the FOLFOX signature in 3,744 colorectal cancer cases from the Caris database (**Table 3**). Cancers with predicted improved benefit from FOLFOX/bevacizumab were more likely to be represented in the CMS2 group, while cancers classified as CMS1 were more frequently predicted to show DB from FOLFOX/bevacizumab treatment.

Discussion

The quality (depth and durability) of a clinical response following first-line chemotherapy in patients with mCRC usually foreshadows

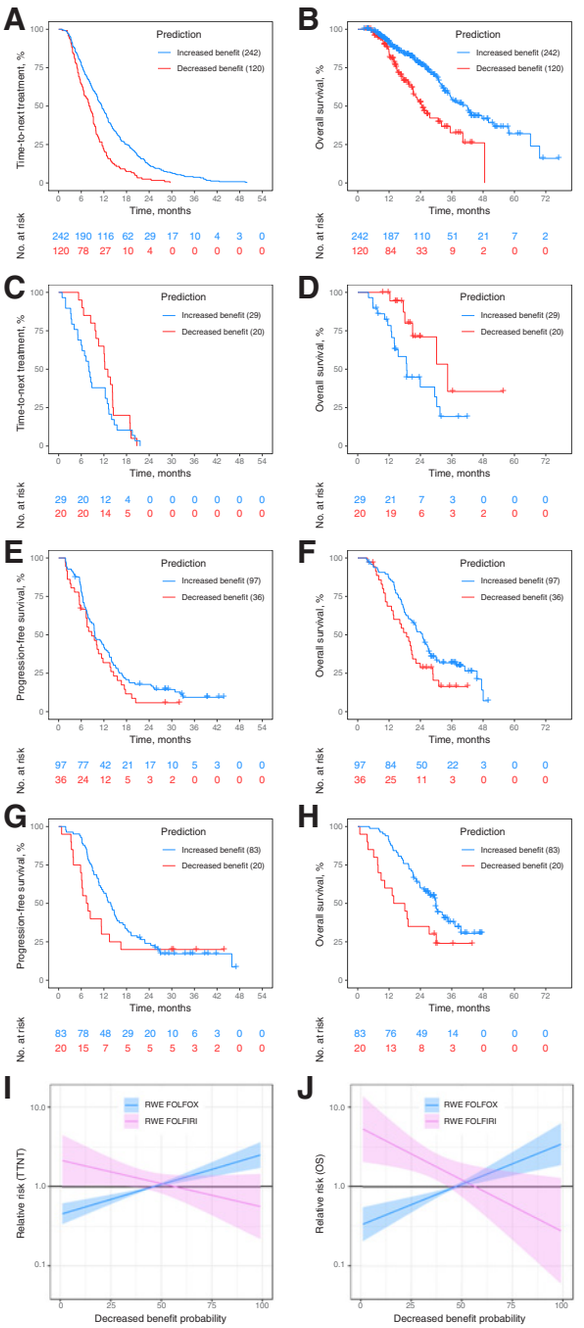

Figure 2.

Blinded RWE testing cohorts that received first-line FOLFOX (**A** and **B**) or first-line FOLFIRI (**C** and **D**), arms A (FOLFOX, **E** and **F**) and B (FOLFOXIRI, **G** and **H**) of the TRIBE2 trial, and RR of MI FOLFOXai scores between the RWE cohorts (**I** and **J**). **A,** The median TTNT in the IB cohort was 3.3 months (40%) longer than the median TTNT in the DB arm (HR, 0.537; 95% CI, 0.428–0.674; log-rank $P < 0.001$). **B,** The median OS in the IB cohort was 17.5 months (71%) longer than the median OS in the DB arm (HR, 0.466; 95% CI, 0.325–0.670; log-rank $P < 0.001$). **C,** The median TTNT in the IB cohort was 4.6 months (36%) shorter than the median TTNT in the DB arm (HR, 1.422; 95% CI, 0.797–2.538; log-rank $P = 0.233$). **D,** The median OS in the IB cohort was 15.7 months (46%) shorter than the median OS in the decreased benefit arm (HR, 2.631; 95% CI, 1.041–6.649; log-rank $P = 0.032$). **E,** The median PFS in the IB cohort was 0.9 months (10%) longer than the median PFS in the decreased benefit arm (HR, 0.757; 95% CI, 0.505–1.135; log-rank $P = 0.18$). **F,** The median OS in the IB cohort was 6 months (32%) longer than the median OS in the DB arm (HR, 0.629; 95% CI, 0.403–0.981; log-rank $P = 0.04$). **G,** The median PFS in the IB cohort was 6.2 months (82%) longer than the median PFS in the DB arm (HR, 0.684; 95% CI, 0.396–1.181; log-rank $P = 0.169$). **H,** The median OS in the IB cohort was 14.1 months (89%) longer than the median OS in the DB arm (HR, 0.483; 95% CI, 0.270–0.864; log-rank $P = 0.02$). RR with respect to TTNT (**I**) and OS (**J**) as a function of DB probability on the patients for which we made a call for both the FOLFOX and FOLFIRI RWE cohorts from a Cox proportional hazards model using DB probability and treatment as the covariates. The intersecting nature of the curves indicates that the DB probability had a different risk effect depending on the treatment received, as evidenced by the reversed signal observed in the RWE FOLFOX (**A** and **B**) and RWE FOLFIRI (**C** and **D**) cohorts.

survival. Because oxaliplatin-associated neuropathy develops by the 4th or 5th month of treatment in most patients and tumors acquire chemotherapy resistance over time, the initial therapeutic impact is particularly important. However, reliable molecular predictors of response to chemotherapy are currently unavailable to inform the choice of initial therapy. With this study, we took advantage of an advanced machine-learning approach to identify and validate FOLFOX*ai*, a molecular signature predictive of treatment benefit from FOLFOX chemotherapy by analyzing a combined dataset of comprehensive molecular profiling results and clinical outcomes data. The key finding of our studies is that FOLFOX*ai* is predictive of OS in patients with mCRC, EC/GEJC, and PDAC, who receive oxaliplatin-containing chemotherapy regimens in first line. To our knowledge, this is the first clinically validated, machine-learning powered molecular predictor of chemotherapy efficacy in these diseases with immediate relevance for the initial therapeutic decision-making process.

Molecular landscape studies, as well as our own data demonstrate an extensive interindividual molecular heterogeneity of mCRC and the presence of up to several thousand mutations per case (18, 19). Thus, it is likely that more than a single mechanism contributes to sensitivity and *de novo* resistance to chemotherapy, a notion that is exemplified by the lack of predictive power for RNA expression level of a single gene (*ERCC1*), which encodes a base excision DNA repair enzyme, as demonstrated in a large, randomized phase II study (7). In contrast, broad molecular characterization of cancers holds the promise of revealing complex systems biology via molecular patterns associated with treatment benefit. Machine-learning algorithms can be instrumental in uncovering such patterns, as it has been demonstrated in the context of radiologic imaging (20). However, machine-learning algorithms as decision support tools for standard treatment decisions in oncology have mostly been limited to cognitive support systems, such as IBM Watson (21), or lack sufficient clinical validation (22, 23).

We applied a two-step clinical validation approach that utilized synthetic study cohorts assembled from RWE data, followed by retrospective-prospective analysis of samples from the TRIBE2 study. Inclusion criteria for the RWE cohorts were modeled after the TRIBE2 study, but maintain some of the variability of treatment schedules observed in daily practice that are not reflected in a randomized clinical trial (24). The validation through the retrospective-prospective analysis of TRIBE2 samples was complementary to the RWE analysis and represents an accepted validation strategy for predictive biomarkers (25). The FOLFOX*ai* signature was able to identify patients on both oxaliplatin-based arms of the randomized TRIBE2 trial who would ultimately have IB, with a clinically relevant increase in OS of 6 months (FOLFOX/bevacizumab arm) or 14.9 months (FOLFIXIRI/

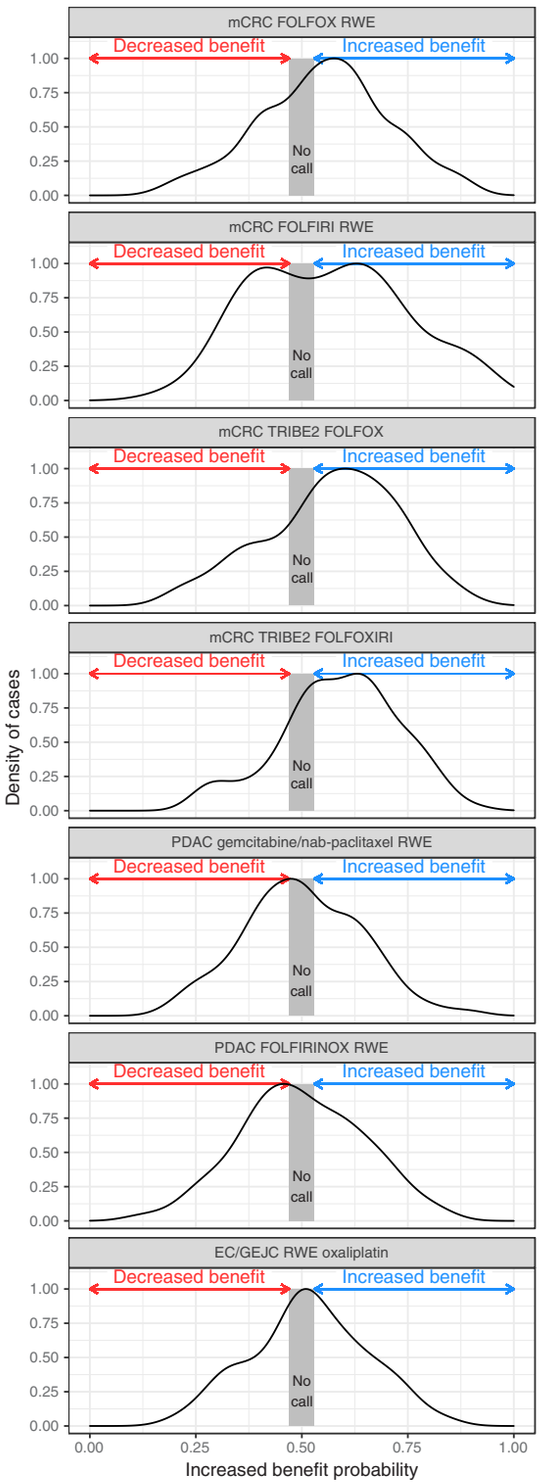

Figure 3.
Density of predictions in the RWE testing cohort and the TRIBE2 trial.

bevacizumab arm). Moreover, the FOLFOX*ai* predicted treatment benefit from FOLFIRI inversely. Therefore, we propose a clinical decision algorithm that utilizes FOLFOX*ai* to prioritize either FOLFOX or FOLFIRI as first-line chemotherapy in patients who are not candidates for the triple-agent FOLFOXIRI regimen and to guide drug discontinuation in case of toxicity in patients receiving FOLFOXIRI as first-line treatment. While these findings suggest incorporation of FOLFOX*ai* in first-line treatment decisions, additional aspects need further consideration. Most importantly, utilization of the signature in the first-line setting requires rapid turn-around times of NGS, signature calculation, and reporting, which Caris Life Sciences has achieved with an average turn-around time of 13.5 calendar days. Furthermore, we were not able to prospectively test whether patients predicted to have DB from FOLFOX will indeed derive greater benefit from FOLFIRI. To address that question formally, a prospective registry study has been implemented.

Our finding that FOLFOX*ai* is also predictive of survival in patients treated with FOLFIRINOX for advanced PDAC highlights the potential extrapolation of this signature to other clinical settings that involve platinum agents and points to potential utility in selecting patients for this more toxic, but nonetheless standard regimen compared with nab-paclitaxel/gemcitabine (9, 26). In concert with our findings in EC/GEJC, these results underscore that FOLFOX*ai* might capture molecular themes relevant for treatment response beyond colorectal cancer, a possibility that is currently under active investigation.

The 67 molecular features included in the signature also provide novel insights into putative biologic mechanisms driving intrinsic resistance to the FOLFOX/bevacizumab or FOLFOX combination. Most notably, factors involved in WNT signaling and mediation of EMT were among the most important features in the signature which are both well known to confer resistance to chemotherapeutic agents (9). For example, BCL9 functions as a transcriptional coactivator of the canonical WNT pathway and has been shown to promote a stem cell–like phenotype (27, 28) that was associated with platinum resistance in non–small cell lung cancer (29). High expression of BCL9 was found to be associated with poor outcome in colorectal cancer, possibly through mediating neuron-like, multicellular communication properties (in addition to its WNT regulatory function; ref. 30).

The CMSs have been demonstrated to be prognostic in mCRC and predictive for the efficacy of biologic agents (11, 17). In the adjuvant setting, the CMS2 subtype has been demonstrated to particularly benefit from FOLFOX chemotherapy (31). In agreement with this, we observed enrichment of CMS2 in the IB cohort. However, our results suggest that FOLFOX*ai* predicts significant portion of CMS1, 3, and 4 patients to also benefit from oxaliplatin-based treatment with metastatic disease, highlighting its independence form currently established molecular classifiers.

In summary, the totality of this work serves as a validation of FOLFOX*ai*, a molecular signature of efficacy of oxaliplatin-based therapy, which is predictive of OS in mCRC. Thus, comprehensive molecular profiling performed at the time of diagnosis of mCRC (and potentially other cancers) not only delivers key information relevant to targeted and immunotherapies, such as mutations in *KRAS, NRAS*, and *BRAF*, MSI status, and HER2 amplification, but also provides crucial guidance for the choice of first-line chemotherapy.

Table 3. Predictions of the algorithm by CMS subtype.

CMS subtype	DB *n* (%)	No call *n* (%)	IB *n* (%)	Total *N* (%)	Predicted DB/no call/IB (%)	*P*[a]	TCGA validation sensitivity (%)
CMS1	280 (29)	62 (13)	228 (10)	570 (15)	49/11/40	<0.001	93.4
CMS2	158 (16)	135 (29)	842 (37)	1,135 (30)	14/12/74	<0.001	88.6
CMS3	160 (16)	60 (13)	318 (14)	538 (14)	30/11/59	0.11	56.7
CMS4	380 (39)	206 (44)	915 (40)	1,501 (40)	25/14/61	0.11	100.0
Total	978	463	2,303	3,744			88.3

[a]χ^2 test.

Authors' Disclosures

J.P. Abraham reports full-time employment with stock from Caris Life Sciences outside the submitted work, as well as has a patent for PCT/US2019/064078 pending and PCT/US2020/035990 pending. D. Magee reports a patent for PCT/US2019/064078 pending and PCT/US2020/035990 pending and full-time employment with stock in Caris Life Sciences. D.D. Halbert reports a patent for PCT/US2019/064078 pending and PCT/US2020/035990 pending and full-time employment with stock in Caris Life Sciences. J. Xiu reports full-time employment with stock from Caris Life Sciences during the conduct of the study and outside the submitted work, as well as has a patent for Caris Life Sciences pending. D.A. Berry reports other from Caris Life Sciences during the conduct of the study and Berry Consultants, LLC outside the submitted work. M.J. Oberley reports employment with Caris Life Sciences. A.F. Shields has been on the Caris Life Sciences' speakers' bureau and has received support for travel and research data analysis. J.L. Marshall reports personal fees from Caris Life Sciences and Indivumed outside the submitted work. M.E. Salem reports other from Taiho Oncology, Pfizer, and QED outside the submitted work. A. Falcone reports grants and personal fees from Amgen, Bayer, Bristol, Daiichi Sankyo, Incyte, Lilly, Merck, MSD, Pierre-Fabre, Roche, and Servier outside the submitted work. A. Grothey reports nonfinancial support from Roche/Genentech, nonfinancial support and other from Bayer, and other from Array/Pfizer and Regeneron outside the submitted work. M.J. Hall reports other from Caris Life Sciences outside the submitted work. H.-J. Lenz reports other from Merck, Bayer, and Roche during the conduct of the study. A. Helmstetter reports full-time employment with Caris Life Sciences and two patents pending. W.M. Korn reports personal fees from Caris Life Sciences (salary and ownership interest) and Merck outside the submitted work, as well as has a patent for PCT/US2019/064078 pending and PCT/US2019/035990 pending. D.B. Spetzler reports a patent for PCT/US2019/064078 pending and PCT/US2020/035990 pending and full-time employment with stock in Caris Life Sciences. No disclosures were reported by the other authors.

Authors' Contributions

J.P. Abraham: Conceptualization, resources, software, formal analysis, validation, investigation, methodology, writing-original draft, project administration, writing-review and editing. **D. Magee:** Software, formal analysis, validation, investigation, methodology, writing-original draft, project administration, writing-review and editing. **C. Cremolini:** Resources, data curation, writing-review and editing. **C. Antoniotti:** Resources, data curation, writing-review and editing. **D.D. Halbert:** Conceptualization, resources, funding acquisition. **J. Xiu:** Data curation, formal analysis, writing-review and editing. **P. Stafford:** Software, investigation, writing-original draft, writing-review and editing. **D.A. Berry:** Investigation, writing-review and editing. **M.J. Oberley:** Writing-review and editing. **A.F. Shields:** Writing-review and editing. **J.L. Marshall:** Writing-review and editing. **M.E. Salem:** Resources, writing-review and editing. **A. Falcone:** Resources, data curation, writing-review and editing. **A. Grothey:** Writing-review and editing. **M.J. Hall:** Writing-review and editing. **A.P. Venook:** Resources, writing-review and editing. **H.-J. Lenz:** Resources, writing-review and editing. **A. Helmstetter:** Software, formal analysis, validation, investigation, visualization, methodology, writing-original draft, writing-review and editing. **W.M. Korn:** Conceptualization, resources, data curation, formal analysis, supervision, funding acquisition, validation, investigation, methodology, writing-original draft, project administration, writing-review and editing. **D.B. Spetzler:** Conceptualization, resources, data curation, software, formal analysis, supervision, funding acquisition, validation, investigation, visualization, methodology, writing-original draft, project administration, writing-review and editing.

Acknowledgments

The authors thank Dr. George Demetri for providing critical review of the article. This work was supported by Caris Life Sciences.

The costs of publication of this article were defrayed in part by the payment of page charges. This article must therefore be hereby marked *advertisement* in accordance with 18 U.S.C. Section 1734 solely to indicate this fact.

Received August 19, 2020; revised October 30, 2020; accepted December 3, 2020; published first December 8, 2020.

References

1. Rothenberg ML, Oza AM, Bigelow RH, Berlin JD, Marshall JL, Ramanathan RK, et al. Superiority of oxaliplatin and fluorouracil-leucovorin compared with either therapy alone in patients with progressive colorectal cancer after irinotecan and fluorouracil-leucovorin: interim results of a phase III trial. J Clin Oncol 2003;21:2059–69.
2. Cremolini C, Antoniotti C, Rossini D, Lonardi S, Loupakis F, Pietrantonio F, et al. Upfront FOLFOXIRI plus bevacizumab and reintroduction after progression versus mFOLFOX6 plus bevacizumab followed by FOLFIRI plus bevacizumab in the treatment of patients with metastatic colorectal cancer (TRIBE2): a multicentre, open-label, phase 3. Lancet Oncol 2020;21:497–507.
3. Amado RG, Wolf M, Peeters M, Van Cutsem E, Siena S, Freeman DJ, et al. Wild-type KRAS is required for panitumumab efficacy in patients with metastatic colorectal cancer. J Clin Oncol 2008;26:1626–34.
4. Kopetz S, Grothey A, Yaeger R, Van Cutsem E, Desai J, Yoshino T, et al. Encorafenib, binimetinib, and cetuximab in BRAF V600E–mutated colorectal cancer. N Engl J Med 2019;381:1632–43.
5. Le DT, Uram JN, Wang H, Bartlett BR, Kemberling H, Eyring AD, et al. PD-1 blockade in tumors with mismatch-repair deficiency. N Engl J Med 2015;372:2509–20.
6. Andre T, Shiu K-K, Kim TW, Jensen BV, Jensen L-H, Punt CJA, et al. Pembrolizumab versus chemotherapy for microsatellite instability-high/mismatch repair deficient metastatic colorectal cancer: the phase 3 KEYNOTE-177 study. J Clin Oncol 38:18s, 2020 (suppl; abstr LBA4).
7. Parikh AR, Lee Fa-C, Yau L, Koh H, Knost J, Mitchell EP, et al. MAVERICC, a randomized, biomarker-stratified, phase II study of mFOLFOX6-Bevacizumab versus FOLFIRI-bevacizumab as first-line chemotherapy in metastatic colorectal cancer. Clin Cancer Res 2019;25:2988–95.
8. Al-Batran SE, Hartmann JT, Probst S, Schmalenberg H, Hollerbach S, Hofheinz R, et al. Phase III trial in metastatic gastroesophageal adenocarcinoma with fluorouracil, leucovorin plus either oxaliplatin or cisplatin: a study of the Arbeitsgemeinschaft Internistische Onkologie. J Clin Oncol 2008;26:1435–42.

9. Conroy T, Desseigne F, Ychou M, Bouché O, Guimbaud R, Bécouarn Y, et al. FOLFIRINOX versus gemcitabine for metastatic pancreatic cancer. N Engl J Med 2011;364:1817–25.
10. Campbell PJ, Getz G, Korbel JO, Stuart JM, Jennings JL, Stein LD, et al. Pan-cancer analysis of whole genomes. Nature 2020;578:82–93.
11. Guinney J, Dienstmann R, Wang X, de Reyniès A, Schlicker A, Soneson C, et al. The consensus molecular subtypes of colorectal cancer. Nat Med 2015; 21:1350–6.
12. Tournigand C, André T, Achille E, Lledo G, Flesh M, Mery-Mignard D, et al. FOLFIRI followed by FOLFOX6 or the reverse sequence in advanced colorectal cancer: a randomized GERCOR study. J Clin Oncol 2004;22:229–37.
13. Salem ME, Puccini A, Grothey A, Raghavan D, Goldberg RM, Xiu J, et al. Landscape of tumor mutation load, mismatch repair deficiency, and PD-L1 expression in a large patient cohort of gastrointestinal cancers. Mol Cancer Res 2018;16:805–12.
14. Abraham J, Spetzler D, Helmstetter A, Korn WM, Magee D. Next generation molecular profiling. Patent WO2020113237. 2020.
15. Patro R, Duggal G, Love MI, Irizarry RA, Kingsford C. Salmon provides fast and bias-aware quantification of transcript expression. Nat Methods 2017;14:417–9.
16. Stintzing S, Wirapati P, Lenz H-J, Neureiter D, Fischer von Weikersthal L, Decker T, et al. Consensus molecular subgroups (CMS) of colorectal cancer (CRC) and first-line efficacy of FOLFIRI plus cetuximab or bevacizumab in the FIRE3 (AIO KRK-0306) trial. Ann Oncol 2019;30:1796–803.
17. Lenz H-J, Ou F-S, Venook AP, Hochster HS, Niedzwiecki D, Goldberg RM, et al. Impact of consensus molecular subtype on survival in patients with metastatic colorectal cancer: results from CALGB/SWOG 80405 (Alliance). J Clin Oncol 2019;37:1876–85.
18. Muzny DM, Bainbridge MN, Chang K, Dinh HH, Drummond JA, Fowler G, et al. Comprehensive molecular characterization of human colon and rectal cancer. Nature 2012;487:330–7.
19. Salem ME, Weinberg BA, Xiu J, El-Deiry WS, Hwang JJ, Gatalica Z, et al. Comparative molecular analyses of left-sided colon, right-sided colon, and rectal cancers. Oncotarget 2017;8:86356–68.
20. Shen Li, Margolies LR, Rothstein JH, Fluder E, McBride R, Sieh W. Deep learning to improve breast cancer detection on screening mammography. Sci Rep 2019;9: 1–12.
21. Somashekhar SP, Sepúlveda M-J, Puglielli S, Norden AD, Shortliffe EH, Rohit Kumar C, et al. Watson for oncology and breast cancer treatment recommendations: agreement with an expert multidisciplinary tumor board. Ann Oncol 2018; 29:418–23.
22. Kaissis G, Ziegelmayer S, Lohöfer F, Steiger K, Algül H, Muckenhuber A, et al. A machine learning algorithm predicts molecular subtypes in pancreatic ductal adenocarcinoma with differential response to gemcitabine-based versus FOLFIRINOX chemotherapy. PLoS One 2019;14:1–16.
23. Mucaki EJ, Zhao JZL, Lizotte DJ, Rogan PK. Predicting responses to platin chemotherapy agents with biochemically-inspired machine learning. Signal Transduct Targeted Ther 2019;4:1.
24. Stewart M, Norden AD, Dreyer N, Henk HJ, Abernethy AP, Chrischilles E, et al. An exploratory analysis of real-world end points for assessing outcomes among immunotherapy-treated patients with advanced non–small-cell lung cancer. JCO Clin Cancer Inform 2019;3:1–15.
25. Parkinson DR, McCormack RT, Keating SM, Gutman SI, Hamilton SR, Mansfield EA, et al. Evidence of clinical utility: an unmet need in molecular diagnostics for patients with cancer. Clin Cancer Res 2014;20:1428–44.
26. Von Hoff DD, Ervin T, Arena FP, Chiorean EG, Infante J, Moore M, et al. Increased survival in pancreatic cancer with nab-paclitaxel plus gemcitabine. N Engl J Med 2013;369:1691–703.
27. de la Roche M, Worm J, Bienz M. The function of BCL9 in Wnt/β-catenin signaling and colorectal cancer cells. BMC Cancer 2008;8:1–13.
28. Deka J, Wiedemann N, Anderle P, Murphy-Seiler F, Bultinck J, Eyckerman S, et al. Bcl9/Bcl9l are critical for Wnt-mediated regulation of stem cell traits in colon epithelium and adenocarcinomas. Cancer Res 2010;70:6619–28.
29. Zhang Yu, Zhang Q, Chen H, Wang C. BCL9 promotes epithelial mesenchymal transition and invasion in cisplatin resistant NSCLC cells via β-catenin pathway. Life Sci 2018;208:284–94.
30. Jiang M, Kang Y, Sewastianik T, Wang J, Tanton H, Alder K, et al. BCL9 provides multi-cellular communication properties in colorectal cancer by interacting with paraspeckle proteins. Nat Commun 2020;11:19.
31. Song N, Pogue-Geile KL, Gavin PG, Yothers G, Kim SR, Johnson NL, et al. Clinical outcome from oxaliplatin treatment in stage II/III colon cancer according to intrinsic subtypes: secondary analysis of NSABP C-07/NRG oncology randomized clinical trial. JAMA Oncol 2016;2:1162–9.